Chemical Science

ROYAL SOCIETY OF CHEMISTRY

EDGE ARTICLE

View Article Online
View Journal | View Issue

Cite this: *Chem. Sci.*, 2020, **11**, 6556

All publication charges for this article have been paid for by the Royal Society of Chemistry

Facile optimization of hierarchical topography and chemistry on magnetically active graphene oxide nanosheets†

Avijit Das,[a] Kousik Maji,[a] Sarajit Naskar[a] and Uttam Manna *[ab]

Highly flexible and two-dimensional (2D) graphene oxide (GO) nanosheets have remained instrumental for developing different functional materials for practically relevant applications. In general, 2D GO is routinely assembled into different structures (*i.e.* layered, porous, *etc.*) for achieving desired properties. However, a facile approach for modifying GO nanosheets with (1) hierarchical topography and (2) desired chemistry is rare in the literature. In this report, adequate optimization of both hierarchical topography and low surface energy chemistry in a confined space (in the order of μm dimensions) of GO nanosheets is unprecedentedly carried out for achieving magnetically active and 2D 'confined-super-water-repellence'. A chemically reactive polymeric complex was covalently deposited on the GO-nanosheets through a facile 1,4-conjugate addition reaction for adopting a chemically reactive and hierarchically featured polymeric interface. Simultaneously, the deposition of iron oxide nanoparticles on the 2D-nanosheets rendered the entire material magnetically active. The post-covalent modification of these chemically/magnetically active and hierarchically featured GO-nanosheets with octadecylamine (ODA) yielded magnetically active and 2D 'confined-superhydrophobicity'. Further, this synthesized material was extended for addressing highly relevant and severe global challenges of 'oil-in-water' and 'water-in-oil' emulsion separation by either selective collection (with an efficiency of above 1000 wt%) of tiny oil-droplets from bulk water or forming magnetically active 'Pickering-type' aqueous droplets, respectively, under various practically relevant harsh conditions, including extremes of pH, salinity, surfactant contamination, *etc.* Further, appropriate functionalization of this chemically/magnetically active 2D nano-interface could be useful in developing functional interfaces for various applications related to energy, catalysis and healthcare.

Received 28th January 2020
Accepted 20th March 2020

DOI: 10.1039/d0sc00517g

rsc.li/chemical-science

Introduction

Optimization of necessary topography and chemistry in two dimensional (2D) graphene oxide (GO) nanosheets remains instrumental for achieving diverse and important properties in synthesized materials having impactful significance in practical settings.[1–5] Inspired by these diverse and rational uses of GO-nanosheets, here, a facile and robust chemical approach has been unprecedentedly introduced for optimizing both the hierarchical topography and desired chemistry in the available space (in the order of μm) of 2D GO nanosheets. Interestingly, the co-optimization of appropriate hierarchical topography and low surface energy chemistry on macro-scale (porous/featureless) objects (that are visible with the naked eye) is imperative for achieving bioinspired extreme liquid wettability.[6–15] In the past, various porous and bulk substrates including polyurethane sponge, fibrous cotton and melamine formaldehyde sponge, were endowed with superhydrophobicity for achieving a very high oil absorption capacity.[16–21] In general, such materials, with a very high absorption capacity, were appropriate for removing the floating and sediment bulk oil phase from aqueous media. However, such a high absorption capacity is not essential for emulsion separation as the content of the oil phase in oil-in-water emulsions is very low. For emulsion separation, the most important requirement is easy accessibility of oil droplets to the oil-absorbent interface in the emulsion solution. In reality, superhydrophobic bulk materials have (i) less available surface area to interact with emulsified oil droplets.

[a]*Bio-Inspired Polymeric Materials Lab, Department of Chemistry, Indian Institute of Technology-Guwahati, Kamrup, Assam 781039, India. E-mail: umanna@iitg.ac.in*
[b]*Centre for Nanotechnology, Indian Institute of Technology-Guwahati, Kamrup, Assam 781039, India*

† Electronic supplementary information (ESI) available: Fig. S1–S23 showing the detailed characterization of MAGO, MACRGO and MASHGO; under oil water wettability of MASHGO; oil/water separation performances of MAGO, MACRGO and MASHGO; absorption capacity of MASHGO; gradual removal of the oil-in-water emulsion by MASHGO, stability of emulsions, oil/water separation at high concentrations of the added surfactant, NMR characterization of oil/water separation; various oil-in-water separations in severe and harsh chemical settings, separation performance for water-in-oil of MASHGO carried out with various oil/oily phases in different chemically complex settings. See DOI: 10.1039/d0sc00517g

Moreover, it is always challenging to (ii) keep a large and bulk superhydrophobic material submerged underwater, as highly porous and spongy superhydrophobic materials loaded with a large amount of trapped air prefer to float on the air/water interface.[18–21] Eventually, the low accessibility of emulsified oil droplets to the bulk superhydrophobic interface is likely to pose a severe challenge in separating different practically relevant and viscous oils (*e.g.* crude oil, vegetable oil, motor oil, *etc.*) from their respective emulsion solutions. Recently, some superhydrophobic sponges were used for early demonstrations of oil/water separation in emulsions that were prepared mostly using organic solvents and oils having the least viscosity (*i.e.*, toluene, hexane, chloroform, gasoline, *etc.*).[16–18] However, such spongy materials would be inappropriate for collecting tiny water droplets from water-in-oil emulsions. Here, a different approach has been introduced for (a) achieving easy accessibility of the oil absorbent interface to the dispersed oil-droplets in oil-in-water emulsions and (b) forming magnetically active 'Pickering type' aqueous droplets to remove the aqueous phase from water-in-oil emulsions. Eventually, emulsified liquid phases were efficiently collected from both oil-in-water and water-in-oil emulsions using superhydrophobic GO nanosheets at practically relevant diverse and severe conditions—including the presence of surfactants, extremes of pH, salinity, *etc.*

In the recent past, the confinement of biomimicked wettability on micrometer scale objects emerged as a promising avenue for various smart applications—including miniaturized chemical reactions, detection of different analytes, confined catalytic activity, contamination-free tiny liquid droplet transport, *etc.* which are otherwise impossible to achieve with the same liquid wettability embedded on macro-scale objects.[22–32] In the past, superhydrophobicity was achieved on microparticles by associating a low surface energy coating through weak chemical bonding/interactions—including metal–thiol bonding, hydrogen bonding, ionic interactions, *etc.* These weak interactions and bondings are less likely to be sustained in practically relevant, diverse and harsh scenarios (*i.e.*, extremes of pH, salinity, *etc.*). Therefore, the previously reported superhydrophobic microparticles are likely to be inappropriate for utilising under practically relevant harsh conditions, including extremes of pH, salinity, surfactant contamination, *etc.*[22–28] Further, the confinement of biomimicked wettability on a flexible and 2D object through facile and robust chemistry could provide a simple basis for developing functional materials for prospective applications in 'real-world' scenarios. In this current report, the rational use of a 1,4-conjugate addition reaction provided a simple and single avenue for co-optimization of both the essential topography and appropriate chemistry on flexible 2D nanosheets. Moreover, the residual chemical reactivity of the confined space in our current design allowed us to associate a wide range of other chemical functionalities through the facile 1,4-conjugate addition reaction under ambient conditions. Further, the association of iron-oxide nanoparticles and appropriate post-modification of the reactive nanocomplex coated GO-nanosheets resulted in achieving magnetically active 'confined-superhydrophobicity' that was capable of performing both in air and under oil.

More importantly, in the past, the submicron particles that displayed either contrasting water wettability or extreme water wettability were extended for proof of concept demonstration of oil-in-water emulsion separation.[23,24,27,29,30] However, the existing challenges of (a) poor oil absorption capacity (below 400 wt%), (b) inability to separate different (cationic, anionic and neutral) surfactant-stabilized emulsions (oil-in-water and water-in-oil) and (c) limited performance in harsh settings are some of the major practical concerns that need to be solved immediately by the prospective use of confined-superhydrophobicity for separating complex forms of various oil/water emulsions in 'real-world' scenarios.[23,24,27,29,30] The currently achieved 2D-confined-superhydrophobicity has been successfully extended for addressing all the above mentioned practically relevant challenges, where the synthesized material not only allowed to soak tiny crude-oil droplets, selectively, from the aqueous phase with a high absorption capacity (above 1000 wt%), but also formed magnetically active 'Pickering-type' droplets for both coalescing and capturing emulsified sub-micron aqueous droplets from water-in-oil emulsions. Moreover, the currently synthesized materials remained highly efficient in (i) separating oil-in-water emulsions stabilized with different types of surfactants (cationic, anionic and neutral), irrespective of both (ii) the size distribution of emulsified oil droplets and (iii) nature of the used oils (*i.e.* crude and refined oils). Furthermore, (iv) such effective oil/water separation performance remained unaltered even under various practically relevant harsh conditions.

Results

Synthesis and characterization of chemically reactive and magnetically active graphene oxide

In the past, two dimensional (2D) graphene oxide nanosheets have been routinely utilized to optimize the essential hierarchical topography on macro-scale objects for adopting superhydrophobicity.[11–15] In contrast to the earlier conventional approaches, here, GO nanosheets were strategically decorated with magnetically active Fe_3O_4 nanoparticles and a chemically reactive porous polymeric coating. In the current design, superhydrophobicity was embedded on the graphene oxide nanosheets having a large surface area and high flexibility for efficient emulsified droplet separation. The large surface area of GO facilitated the interaction between the superhydrophobic interface and emulsion droplets, and the flexibility of GO allowed better arrangement around the water droplets in the oil phase of the water-in-oil emulsion. Eventually, rapid and efficient oil-in-water and water-in-oil emulsion separation was achieved. Firstly, magnetically active amino-graphene oxide (MAGO) was synthesized by depositing Fe_3O_4 nanoparticles on nitro-graphene oxide nanosheets (see the ESI† for the detailed procedure). The successful deposition of Fe_3O_4 nanoparticles was confirmed by transmission electron microscopy (TEM) imaging, Fourier-transform infrared spectroscopic (FTIR) analysis and X-ray photoelectron spectroscopy (XPS) characterization as shown in Fig. S1.† The FTIR spectra of MAGO revealed the existence of a strong broad peak at 590 cm^{-1} corresponding to the Fe–O bond (Fig. S1G†) which clearly indicated the

successful oxidation of the Fe^{2+} ions to Fe_3O_4. During the course of this chemical reaction, the nitro-graphene oxide was reduced to amino graphene oxide as evident from the appearance of an IR peak at 1610 cm^{-1} corresponding to the N–H bending of primary amine (Fig. S1G†). In the MAGO, Fe_3O_4 is most likely to interact with the hydroxyl and amine group of the amino graphene oxide through co-ordination/hydrogen bonds. Additionally, the TEM images of MAGO clearly confirmed the deposition of Fe_3O_4 nanoparticles (Fig. S1B†) with a lattice spacing of 0.29 nm which corresponds to the (100) plane of the deposited Fe_3O_4 nanoparticles on the GO nanosheets as characterized with high-resolution transmission electron microscopy (HRTEM) imaging (Fig. S1C†). Energy-dispersive X-ray spectroscopic (EDX) analysis also confirmed the existence of Fe element (61.5 wt%) in the MAGO as shown in Fig. S2.† Thereafter, a chemically reactive polymeric complex,[33,34] synthesized by mixing of BPEI and 5Acl under ambient conditions (Scheme 1A), was covalently integrated into MAGO. The amine groups of MAGO readily reacted with the residual acrylate groups of the polymeric complex under ambient conditions through the 1,4-conjugate addition reaction, and eventually yielded chemically reactive and magnetically active hierarchically featured GO nanosheets (CRMAGO) as shown in Scheme 1B and C. The surface topography, residual chemical reactivity and magnetic properties of the synthesized CRMAGO were thoroughly characterized as shown in Fig. 1.

The comparison of field emission scanning electron microscopy (FESEM) images between MAGO and CRMAGO confirmed the successful immobilization of the polymeric complex as shown in Fig. 1A–D. The random aggregation of the granular polymeric complex contributed towards the construction of hierarchical topography which is essential for exhibiting extreme water repellence. Further, the existence of residual chemical reactivity in the CRMAGO was investigated following the standard and widely accepted FTIR spectral analysis. In the FTIR spectra (Fig. 1E), the appearance of IR peaks at 1409 cm^{-1} and 1735 cm^{-1} for the C–H deformation of the β-carbon of the vinyl groups and carbonyl stretching, respectively, validated the presence of residual acrylate groups—which are capable of reacting with alkylamines under ambient conditions.

Achievement of confined superhydrophobicity by post covalent modification of CRMAGO

As expected, the post-chemical modification of the CRMAGO with octadecylamine (ODA) resulted in depletion of IR peak intensity at 1409 cm^{-1} with respect to the IR peak at 1735 cm^{-1} (served as the internal reference). During the 1,4-conjugate addition reaction between amine and acrylate groups, only the

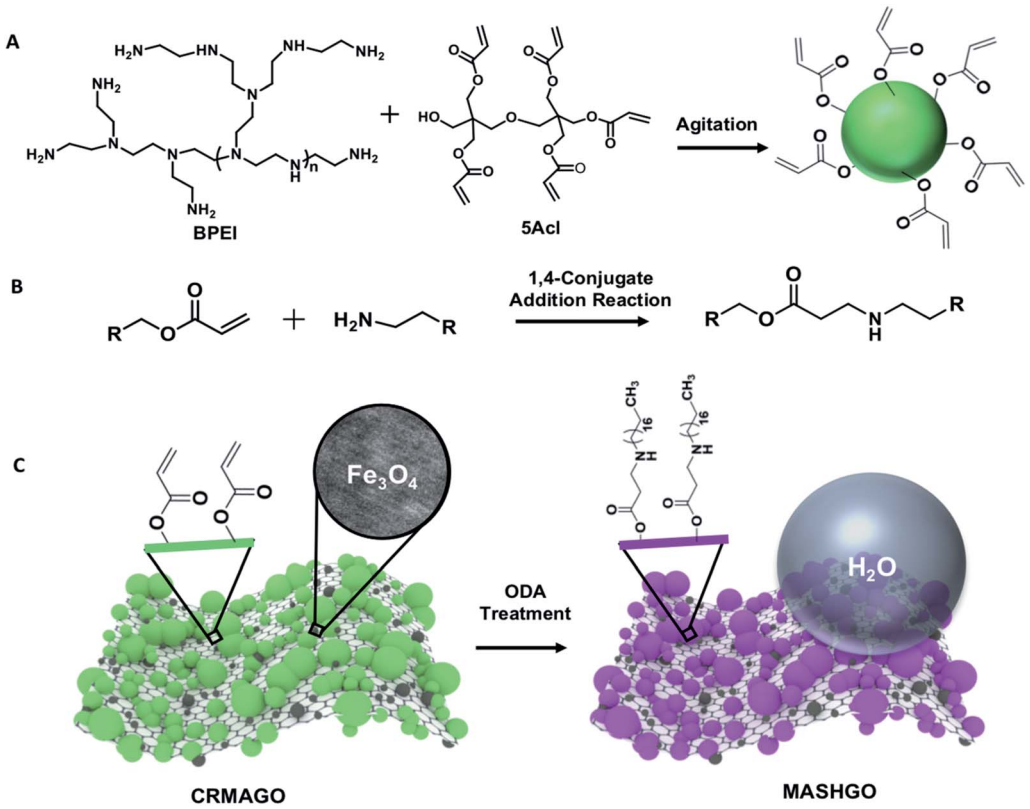

Scheme 1 (A) Schematic illustration of the formation of the chemically reactive polymeric complex prepared by mixing of branched polyethylenimine (BPEI) and dipentaerythritol pentaacrylate (5Acl) under ambient conditions. During the polymeric nanocomplex formation, BPEI and 5Acl covalently crosslinked through the 1,4 conjugate addition reaction between acrylate and primary amine groups (B). (C) Schematic representation of chemically reactive, magneticallyactive and hierarchically featured graphene oxide (CRMAGO), and further post modification with octadecylamine (ODA) provided magnetically active and confined-superhydrophobicity.

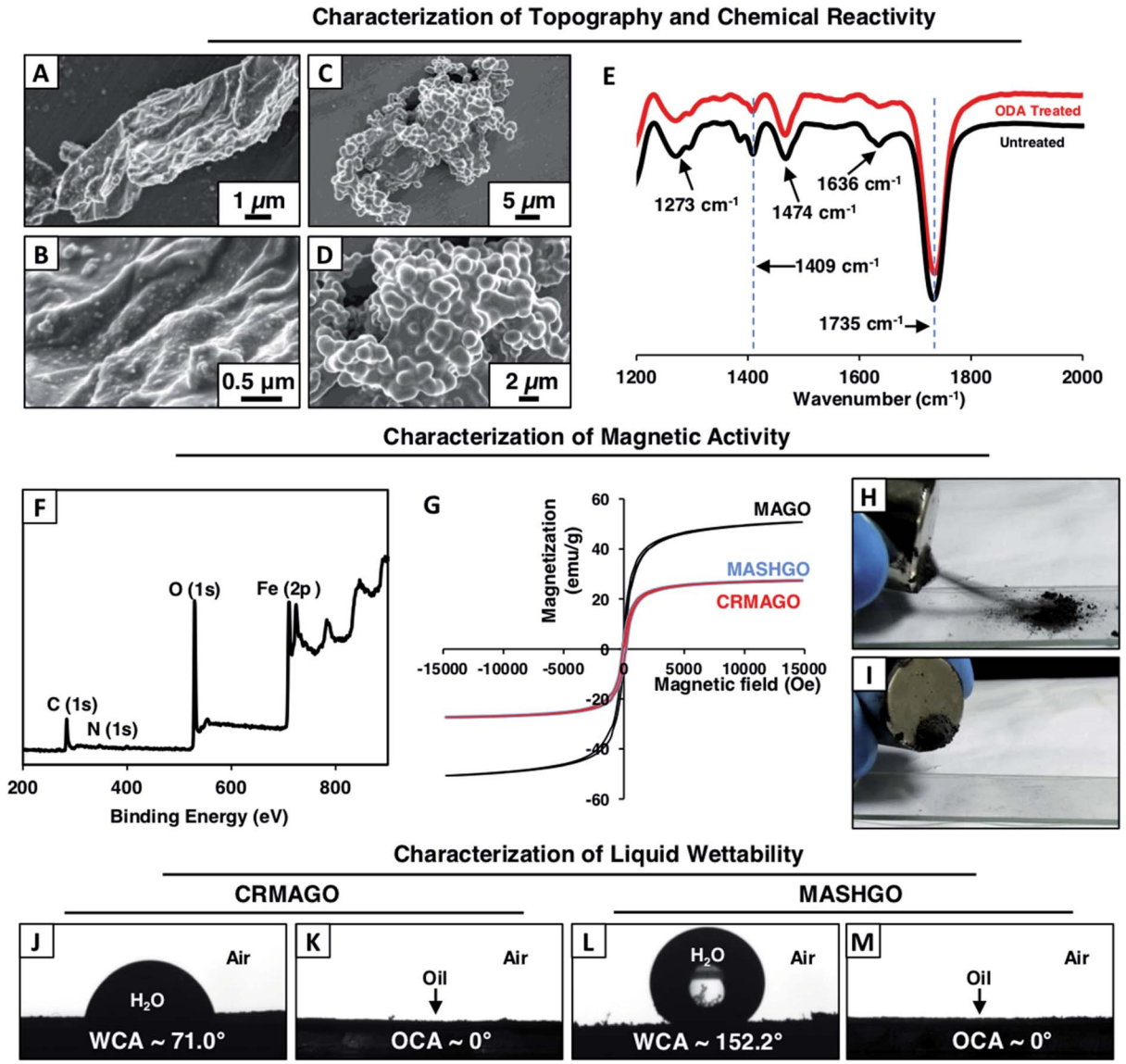

Fig. 1 (A–D) FESEM images of magnetically active graphene oxide (MAGO; (A and B)) and magnetically active superhydrophobic graphene oxide (MASHGO; (C and D)) in low (A and C) and high magnifications (B and D). (E) FTIR spectra of the chemically reactive and magnetically active graphene oxide (CRMAGO) before (black) and after (red) ODA treatment. In the FTIR spectra, the IR peak at 1735 cm^{-1} corresponds to C=O stretching. IR peaks at 1636 cm^{-1}, 1474 cm^{-1}, 1409 cm^{-1} and 1273 cm^{-1} are characteristic IR signatures for C=C stretching, C–H bending of the methylene group, C–H deformation of the β-carbon of the vinyl group and the C–O stretching of the ester group, respectively. (F) XPS spectra of MAGO. (G) Magnetization curves of MAGO (black), CRMAGO (red) and MASHGO (blue) at room temperature. (H and I) Digital images illustrating the collection of MASHGO usingh a neodymium magnet (0.5 T). (J–M) Static contact angle images of beaded water (J and L) and oil (K and M) droplets on CRMAGO (J and K) and MASHGO (L and M).

vinyl moiety of the acrylate groups were consumed—and the carbonyl moiety of the acrylate groups remained unaffected (Fig. 1E). The successful post covalent modification of the CRMAGO with ODA altered the water wettability resulting in transition from hydrophilicity (with a water contact angle of ~71°) to superhydrophobicity with a water contact angle of ~152°; however, the extreme oil affinity (with an oil contact angle of 0°) of the material remained intact as shown in Fig. 1J, M and S3.† Further, the extreme water repellency of the synthesized material remained intact in the oil/oily phase as shown in Fig. S4A and B.† This uninterrupted superhydrophobicity under oil contributed to the formation of magnetically active 'Pickering type' droplets in the oil phase and this principle might be effectively used for easy separation of aqueous contaminants from jet-engine fuel.

Next, the embedded magnetic properties in the synthesized material were thoroughly characterized using a vibrating sample magnetometer (VSM). The successful deposition of Fe_3O_4 nanoparticles on MAGO was reconfirmed by XPS analysis as shown in Fig. 1F, where the appearance of binding energy peaks at 726.0 eV and 711.7 eV for Fe $2p_{1/2}$ and Fe $2p_{3/2}$, unambiguously revalidated the successful deposition of Fe_3O_4

nanoparticles on MAGO.[35] The MAGO displayed a paramagnetic behavior with a S-shape magnetic hysteresis curve and a magnetic saturation value (M_s) of 50.7 emu g^{-1} as shown in Fig. 1G. As expected, a change in the magnetic properties was clearly noted after depositing the chemically reactive hierarchical polymeric coating on MAGO. Nevertheless, the CRMAGO still remained highly paramagnetic with a magnetic saturation value of 27.3 emu g^{-1} as shown in Fig. 1G. After the post-covalent modification of CRMAGO with ODA, the magnetic properties remained unaltered as noted in Fig. 1G (blue line). Thus, magnetically active and superhydrophobic graphene oxide (MASHGO) was successfully synthesized. Furthermore, a lab used magnet (nickel coated neodymium magnet 0.5 T) when brought in close proximity to the material, immediately attracted the entire superhydrophobic GO powder as shown in Fig. 1H, I and Movie 1.† This MASHGO was further extended for addressing challenges related to comprehensive remediation of both oil-in-water and water-in-oil emulsion solutions, irrespective of the size distribution of emulsified droplets, under various practically relevant harsh conditions, including extremes of pH, salinity, surfactant contamination, *etc.*

Oil-in-water/water-in-oil emulsion separation in challenging settings

Regular off-shore bulk crude oil spill accidents and uncontrolled discharge of emulsified industrial wastewater are growing concerns as oil contamination in open water reservoirs pose a severe global threat to the aqua eco-system. In the past, bio-inspired superhydrophobic sponges and membranes were successfully used for selective absorption and filtration based 'bulk'-oil separation from oil/water mixtures.[36–40] However, the superhydrophobicity embedded on these macro-scale objects (sponge and mesh) is fundamentally inappropriate for remediating tiny oil-in-water emulsion droplets as the bulk aqueous phase prevents the access of submicron oil droplets to the selective superoleophilic interfaces. In addition to this, the coating of various chemicals—including asphaltenes, resins, and naphthenic acids around the crude oil droplets pose a severe challenge to oil/water separation; unlike other emulsions that are made out of refined oils.[41] Thus, the design of a single high throughput approach for separation of both water-in-oil and oil-in-water emulsions in practically relevant harsh and challenging settings is extremely important for the efficient remediation of oil/oily pollutants. As a proof of concept demonstration, firstly, the synthesized MASHGO was placed at the crude oil/water interface where it selectively absorbed the floating oil phase from the aqueous phase. The oil absorbed MASHGO was collected from the air/water interface using a neodymium magnet that is wrapped in cotton fabric as shown in Fig. S5 and Movie 2.† The oil absorption capacity of the MASHGO was measured to be above 1000 wt% which was significantly higher than that of the reported superhydrophobic/Janus particles.[23,24,27,29,30] Further, the wrapped cotton fabric on the magnet was removed and manually squeezed to recollect the absorbed oil phase as shown in Fig. S5.† The same MASHGO could be reused for oil/water separation after ethanol-washing followed by air-drying. The selective oil-absorption capacity remained mostly unaffected even after 50 times of successive use for oil/water separation (Fig. S6†) and the extreme water repellence also remained unaltered. Further, this selective oil absorption performance remained unaffected, irrespective of the nature of oil/oily phases (*i.e.* petrol, diesel and veg oil; Fig. S7A†) used for preparing the respective oil/water mixtures. However, both the MAGO and CRMAGO failed to separate the oil phase completely from the aqueous phase (Fig. S8A–R†) as the oil absorption ability of both the MAGO and CRMAGO was found to be significantly low as compared to that of MASHGO as shown in Fig. S7A.† This simple study confirmed that the 2D confined-superhydrophobicity was instrumental for selective and repetitive absorption of oil/oily contaminants from the aqueous phase with a high absorption capacity. Moreover, the performance of the MASHGO remained indistinguishable even in practically relevant challenging settings, including extremes of pH, seawater and river water (Fig. S7B†).

Next, the MASHGO was rationally applied to separate both the oil-in-water and water-in-oil emulsions by either selective absorption of the oil phase or forming *in situ* magnetically active 'Pickering-type' aqueous droplets, respectively. At first, a solution of the crude oil-in-water emulsion (2% v/v) was prepared, where water-immiscible Nile red dye added crude oil aided both visual inspection and fluorescence microscopy characterization. This emulsion solution remained stable, and the size distribution of the oil-in-water emulsion remained unaltered even after 24 h as monitored with DLS study in Fig. S9.† Both the formation of emulsified oil droplets (with an average size of 1 μm) in the bulk aqueous phase and the removal of the same oil droplets after treatment with MASHGO were characterized through visual inspection, fluorescence microscopy imaging and dynamic light scattering (DLS) study (Fig. 2A–L).

Two separate vials of the same crude-oil-in-water emulsion solution in the presence (right-side vial) and absence (left-side vial) of added MASHGO were agitated vigorously for 2.5 minutes (Movie 3†), where the agitation paved the way towards easy access of emulsified oil droplets to MASHGO. With time, the fluorescence dye added emulsified oil droplets which aided in scattering light was selectively absorbed on MASHGO and the transmittance of the highly opaque, brown-colored emulsion solution significantly improved. After 2.5 minutes, the opaque, brown-colored emulsion became colorless and completely optically transparent (Fig. 2G, H, K, and S10†), where an external magnet is applied to separate MASHGO from emulsion solution prior to measuring the transmittance. At the end, an oil-free aqueous phase was obtained on the application of the external magnet (nickel coated neodymium magnet, 0.5 T) as shown in Fig. 2G and as confirmed with fluorescence microscopy imaging (Fig. 2H), dynamic light scattering (DLS) study (Fig. 2L) and ^{1}H-NMR analysis (Fig. S11†). The selective soaking of crude-oil by the aggregated MASHGO was confirmed *via* fluorescence imaging in Fig. 2F, whereas, such a drastic change was not observed for the emulsion solution in the absence of MASHGO (Fig. 2E). As expected, both the MAGO and CRMAGO remained incapable of separating crude oil-droplets from the

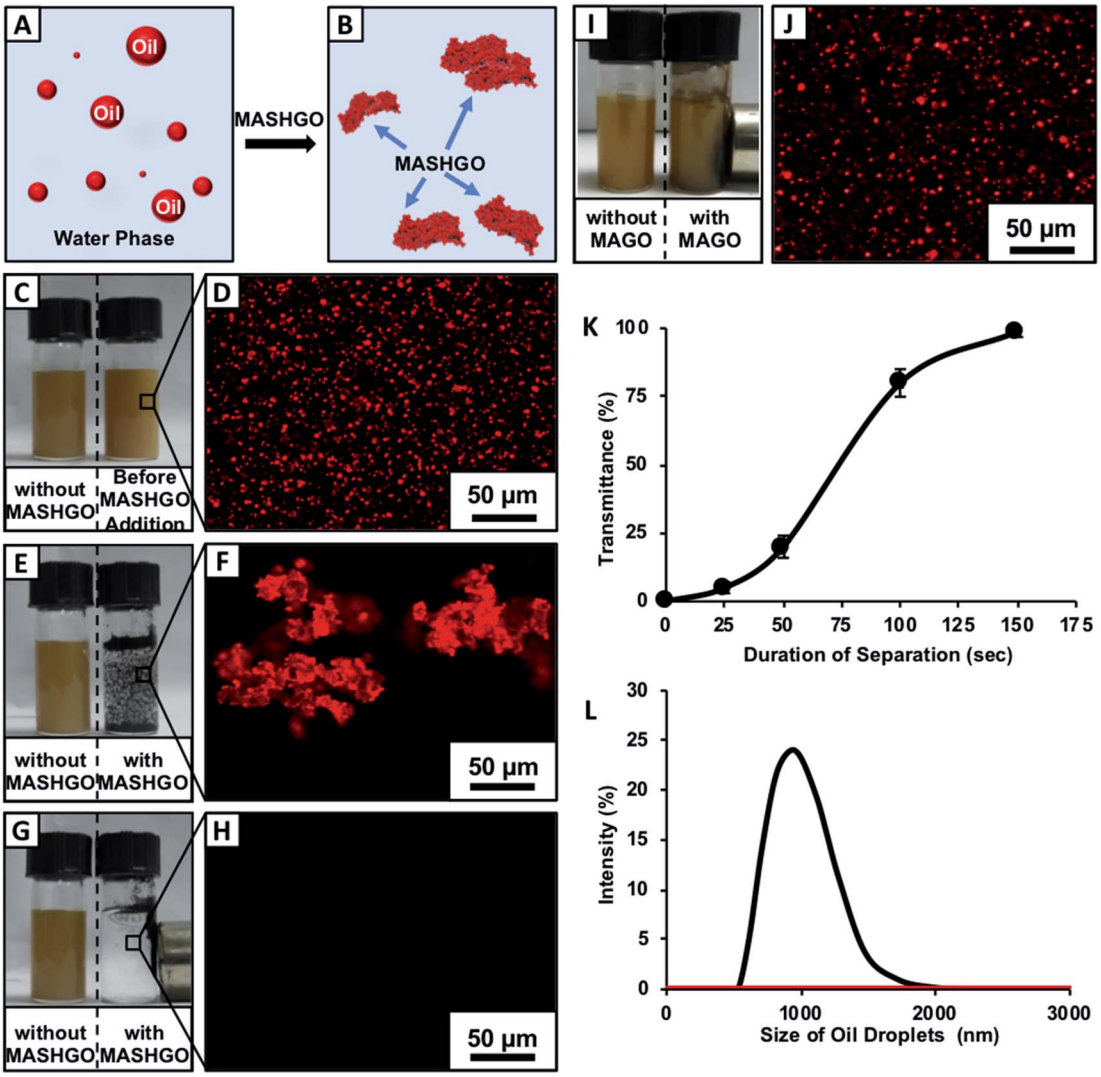

Fig. 2 (A and B) Illustrations of the selective absorption of tiny crude oil droplets by magnetically-active superhydrophobic graphene oxide (MASHGO) from the water phase. (C–H) Digital images (C, E and G) and fluorescence microscopy images (D, F and H) demonstrating crude oil-in-water emulsion separation ability of MASHGO, where the crude oil is labelled with Nile red. (C, E and G) Two separate vials of crude oil-in-water emulsions with (right-side vial) and without (left-side vial) MASHGO were agitated for 150 seconds (C and E) before the application of a nickel coated neodymium magnet (G). (I and J) Digital image (I) and fluorescence microscopy image (J) demonstrating the failure of MAGO in separation of the oil-in-water emulsion. (K) A plot showing the change in transmittance (%) of the crude oil-in-water emulsion solution in the presence of MASHGO, where transmittance is recorded after the application of the external magnet. (L) DLS study on the crude oil-in-water emulsion before (black) and after (red) performing oil/water separation by MASHGO.

oil-in-water emulsion as shown in Fig. S12,† 2I and J. The 2D confined-superhydrophobicity played a crucial role in the successful and rapid separation of oil/water from oil-in-water emulsions. Moreover, the oil/water separation performance by the MASHGO remained intact even on increasing the percentage of crude-oil in the respective oil-in-water emulsion as shown in Fig. S13.† Again, this emulsified crude oil separation ability by the MASHGO remained unaltered in different harsh aqueous environments including high pH, low pH, seawater, and river water (Brahmaputra, Guwahati, Assam, India) as shown in Fig. S14.† Further, various natural and synthetic oils, which produce oil–water emulsions with different size distributions of oil droplets were also successfully separated using MASHGO as confirmed by visual inspection, DLS study and fluorescence microscopy imaging (Fig. S15†). The synthesized material remained efficient for the repetitive separation of the oil-in-water emulsion, for at least 50 times. Moreover, the separation of the surfactant stabilized oil-in-water emulsion is a severe challenge, due to the existence of a protective layer of surfactant around the oil/oily droplets. In this current study, the same MASHGO was also extended for separating different surfactant stabilized oil-in-water emulsions. The synthesized MASHGO displayed an unparalleled ability for separating oil/water in different types of surfactant-stabilized oil-in-water emulsions. The respective emulsions were prepared in the presence of a positively charged surfactant (CTAB, a concentration of 1 mM), negatively charged surfactant (SDS, a concentration of 1 mM) and non-ionic surfactant

(Triton-X, a concentration of 1 mM) as shown in Fig. 3 and S16.† Visual inspection, fluorescence imaging and DLS study unambiguously confirmed the successful removal of crude oil droplets from their respective surfactant stabilized emulsions. Thus, the confined superhydrophobicity on GO nanosheets played an important role in the comprehensive remediation of oil spillages in practically relevant challenging settings. Even, the crude-oil-(2%)-in-water emulsion was successfully separated using MASHGO in the presence of highly concentrated (10 mM, above CMC) SDS solution as shown in Fig. S17.†

The application of the same MASHGO powder allowed the successful separation of micron/submicron-sized water droplets from various bulk oil phases as schematically demonstrated in Fig. 4A and B. For the proof of concept demonstration, a water-in-oil emulsion (2% v/v) was prepared by mixing of the fluorescein dyed aqueous phase in kerosene followed by continuous sonication for 1 hour. Fluorescence microscopy and DLS study of the emulsion confirmed the formation of micron/submicron-sized water droplets in kerosene and these aqueous droplets remained homogeneously suspended in the oil phase for several hours (Fig. 4C and D). However, the agitated water-in-oil emulsion in the presence of MASHGO formed magnetically active 'Pickering-type' droplets, where the 2D MASHGO sheets facilitated the coalescence of submicron water droplets in the oil phase as shown in Fig. 4E, F and S18.† Further, the fluorescence microscopy images revalidated the formation of the 'Pickering-type' emulsion where the non-fluorescent and black MASHGO sheets were wrapped around the large and fluorescent aqueous droplets as shown in Fig. 4F. The inherent tendency of the synthesized MASHGO towards extreme water repellence in the oil phase provided the basis of forming a 'Pickering-type' droplet as similar to the dry liquid marbles in air. Further, the hydrophobic particles have an energetic preference to settle at the water–oil interface of the water-in-oil emulsion and form the Pickering emulsion.[42] Further, these MASHGO wrapped water droplets were easily removed from kerosene by the application of an external magnet as shown in Fig. 4G and Movie 4.† Eventually, a completely clean oil phase with 100% transmittance was recovered (Fig. S19†). Moreover, visual inspection (Fig. 4G), fluorescence microscopy imaging (Fig. 4H) and the DLS study (Fig. 4J) revalidated this successful removal of aqueous contaminants from the oil phase by the MASHGO. This oil/water separation performance remained unperturbed even on increasing the amount of aqueous phase in the respective water-in-oil emulsion as

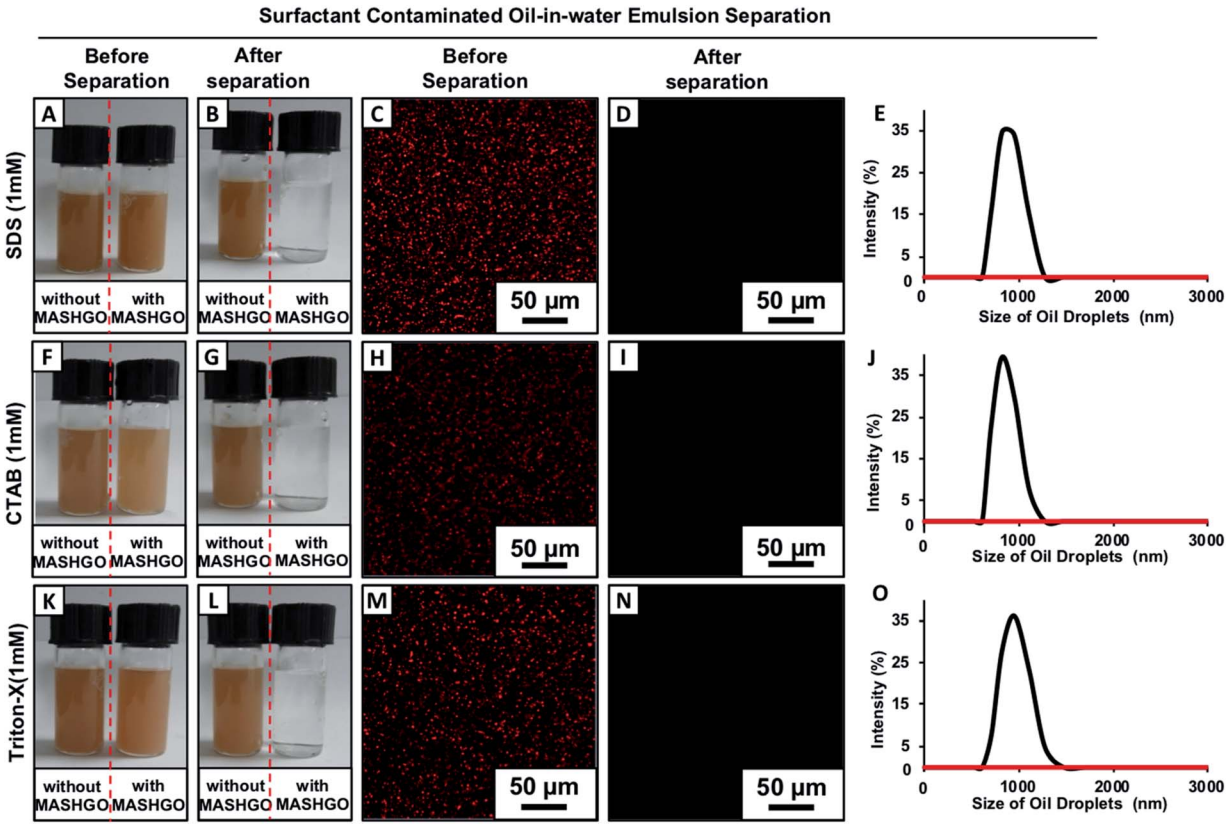

Fig. 3 ((A and B), (F and G) and (K and L)) Digital images of the crude oil-in-water emulsion before (A, F and K), and after (B, G and L) oil/water separation by MASHGO in the presence of anionic (SDS), cationic (CTAB) and neutral (Triton-X) surfactants. The left-side and right-side vials with the dotted red lines denote crude oil-in-water emulsions without and with MASHGO, respectively. ((C and D), (H and I) and (M and N)) Fluorescence microscope images of the crude oil-in-water emulsion before (C, H and M) and after (D, I and N) oil/water separation by MASHGO in the presence of different surfactants. (E, J and O) DLS plots of the crude oil-in-water emulsion before (black) and after (red) oil/water separation by MASHGO in the presence of different surfactants.

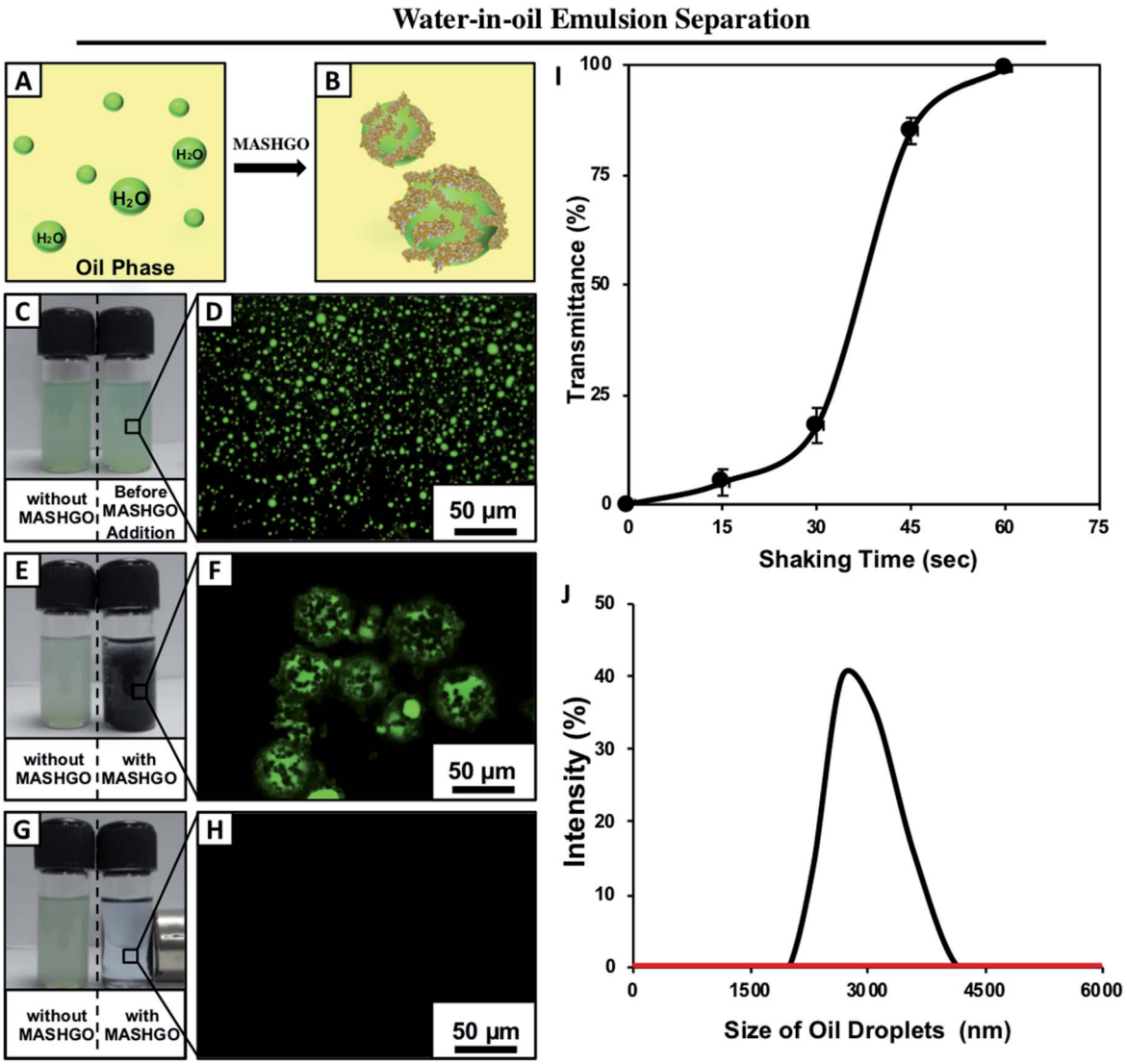

Fig. 4 (A and B) Schematic illustrating the formation of magnetically active 'Pickering type' droplets in the water-in-oil emulsion in the presence of MASHGO. (C–H) Digital images (C, E and G) and fluorescence microscopy images (D, F and H) representing the water-in-kerosene oil emulsion before addition of MASHGO (C and D), after addition of MASHGO (E and F) and after the application of the external magnet (G and H). (E and G) Digital images of two separate vials of the same water-in-kerosene oil emulsion solutions in the presence (right-side vial) or absence (left-side vial) of added MASHGO. (I) A plot showing the change in transmittance (%) of the water-in-oil emulsion solution in the presence of MASHGO during the course of oil/water separation, where the transmittance is recorded after application of the external magnet. (J) DLS study on the water-in-oil emulsion before (black) and after (red) performing oil/water separation by MASHGO.

shown in Fig. S20.† Moreover, the performance of oil/water separation from the water-in-oil emulsion by MASHGO remained unaltered for different types of oil phases (*e.g.* veg oil, petrol, diesel, and bio-fuel) (Fig. S21†), irrespective of the nature of chemical complexity of the aqueous phase (*e.g.* acidic water, basic water, seawater, river water and surfactant contaminated water) as shown in Fig. S22 and S23.†

Conclusions

In this report, a chemically reactive, magnetically active and hierarchically featured coating was introduced on individual GO nanosheets following a simple and robust chemical approach for achieving two dimensional (2D) magnetically active confined-superhydrophobicity. The synthesized MASHGO was highly capable of separating oil/water from both oil-in-water and water-in-oil emulsions, irrespective of the nature of the oil used for preparing emulsions and even in the presence of practically relevant chemically complex scenarios—including extremes of pH, sea-water, *etc.* Moreover, this current approach was efficient for the rapid separation of submicron-oil droplets stablilized with different surfactants. Further, the oil/water separation performance remained unaltered irrespective of the size distributions of micron/sub-micron liquid droplets in the respective emulsions either by selective absorption of oil droplets (in the aqueous phase) or formation of magnetically active 'Pickering-type' aqueous droplets in the oil phase. Therefore, confined superhydrophobicity on 2D nanosheets can be envisioned as a promising and facile

approach for high through-put cleaning of oil spills, fuel purification, *etc.* Further, this chemically and magnetically active design of GO nanosheets could be useful in developing various functional materials by adopting appropriate post-covalent modification through the 1,4-conjugate addition reaction.

Experimental

Materials

Dipentaerythritol penta-acrylate (5Acl, M_w = 524.21 g mol^{-1}), branched polyethyleneimine (BPEI, M_w = 25 kg mol^{-1}), and octadecylamine were obtained from Sigma Aldrich, Bangalore, India. Graphite powder, rhodamine 6G and fluorescein were acquired from Labo Chemie, Mumbai, India. Ethanol, sodium hydroxide, ammonium hydroxide, hydrazine hydrate, hydrogen peroxide, sulphuric acid, hydrochloric acid, and nitric acid were procured from Merck Specialties Private Limited, India. Potassium permanganate was procured from Fisher scientific. Nile red was purchased from Tokyo Chemical Industry Co., Ltd. Iron(II) chloride tetrahydrate was purchased from Alfa Aesar, India. Vegetable oil, petrol, diesel, kerosene and a nickel neodymium magnet were purchased from a local shop in Guwahati city (Assam, India). Crude oil was obtained from Indian Oil Corporation Limited, Guwahati.

General considerations

The liquid wettability was characterized using a KRUSS Drop Shape Analyser-DSA25 at 20 °C temperature, where 5 μL of deionized (DI) probe liquid droplets were used for measuring the contact angle. All dynamic light scattering (DLS) study measurements were conducted using a Zetasizer Nano ZS90 instrument (model no. ZEN3690). FTIR spectra were recorded using a PerkinElmer instrument under ambient conditions by preparing KBr pellets. Electron microscopy images and energy-dispersive X-ray (EDX) analysis spectra were collected using a Carl Zeiss field emission scanning electron microscope (FESEM). All Raman spectra were recorded using a Laser Micro Raman System (Horiba Jobin Vyon, Model LabRam HR). The magnetic properties of synthesized materials were investigated by using a vibrating sample magnetometer (Make: Lakeshore, Model: 7410 series). A field emission transmission electron microscope (Make: JEOL, Model: 2100F) was used for characterizing the deposition of iron oxide. XRD spectra were recorded using an X-ray diffractometer (Make: Rigaku, Model: Micromax-007HF). All digital pictures and videos were captured with a Canon PowerShot SX420 IS digital camera. All optical microscopy images were recorded using a Confocal Laser Scanning Microscope (CLSM) (Make: Zeiss, Model: LSM 510Meta). All NMR data were collected using a 400 MHz Nuclear Magnetic Resonance (NMR) Spectrometer (Make: Varian, Model: Mercury Plus). XPS spectra were obtained using an X-ray Photoelectron Spectrometer (Make: Thermo Fisher Scientific Pvt. Ltd., UK, Model: ESCALAB Xi+).

Synthesis of graphene oxide (GO)

Graphene oxide (GO) was synthesized by using a modified Hummers method.[43] Briefly, 1 g of graphite powder was added into 50 ml of concentrated sulphuric acid at 0 °C and the whole solution was kept under continuous agitation for 1 h. Then, 6 g potassium permanganate was slowly added into the reaction mixture of concentrated sulphuric acid and graphite powder while maintaining the temperature of the reaction solution below 10 °C. Thereafter, the mixture was kept under continuous agitation for two hours and the temperature was gradually increased to 35 °C. After that, the reaction mixture was placed in an ice bath and diluted with 100 ml of water. Then, 8 ml of 30% hydrogen peroxide was added and the reaction mixture was kept as such overnight. The obtained graphene oxide was thoroughly washed with 20% HCl followed by acetone and was dried under vacuum.

Synthesis of magnetically active amino-graphene oxide (MAGO)

200 mg of graphene oxide (GO) powder was added to 200 ml of 50% nitric acid. Then, the solution of GO was kept for 24 h at room temperature with continuous agitation for preparing nitro-graphene oxide (NGO). Later, the reaction mixture was thoroughly washed with water and acetone followed by drying under vacuum. Thereafter, freshly prepared NGO (80 mg) was dispersed in 30 ml water by sonication. Then, 160 mg iron(II) chloride tetrahydrate was added to the solution with continuous agitation for 30 minutes at room temperature. Next, 1 ml of hydrazine hydrate was added to the reaction solution followed by the addition of 1 ml of ammonia solution (25%) to make the solution alkaline with constant stirring. The solution was kept under continuous agitation for 4 h, and then, the temperature was gradually increased to 70 °C. The solution was allowed to attain room temperature and the magnetically active amino-GO (MAGO) sheets were collected by the application of a nickel coated neodymium magnet. The separated MAGO sheets were thoroughly washed with water and acetone several times and finally dried under vacuum.

Synthesis of chemically reactive and magnetically active graphene oxide (CRMAGO)

At first, solutions of BPEI (0.105 M with respect to the polymer repeat unit) and 5-Acl (0.084 M) were prepared separately in methanol. Then, 125 mg MAGO was dispersed in (15 ml) of the 5-Acl solution by sonication followed by the addition of 1 ml of ammoniacal (25 μL of NH_3) BPEI solution. Then the reaction mixture was kept for 1 h under continuous agitation for the formation and *in situ* deposition of a chemically reactive polymeric complex on MAGO. At the end, a chemically reactive and magnetically active graphene oxide (CRMAGO) was collected using a neodymium magnet, and the synthesized material was thoroughly washed with THF 5 times and finally dried in a vacuum.

Synthesis of magnetically active 2D superhydrophobic graphene oxide (MASHGO)

The residual acrylate groups in the as-synthesized CRMAGO were further reacted with octadecylamine (ODA) through the 1,4-conjugate addition reaction to achieve a magnetically active

and superhydrophobic graphene oxide (MASHGO). At first, a solution of octadecylamine (10 mM) was prepared in an ethanol medium. Then, dried CRMAGO was immersed in the solution for 8 h at room temperature. After the post-chemical modification, the material was thoroughly washed with ethanol several times. After vacuum-drying, the embedded superhydrophobicity was characterized through visual inspection and contact angle measurements.

Separation of the bulk floating oil phase from the aqueous phase

Synthesized MASHGO powder (50 mg) was placed on and around the floating oil phase (1 ml). Immediately, the floating oil phase on the water phase was selectively absorbed by the MASHGO powder. Next, a neodymium magnet which was wrapped with cotton fabric was used to re-collect the MASHGO. During this process, both the floating crude oil and MASHGO were separated and collected from the aqueous phase. The used MASHGO was washed with ethanol and dried in a vacuum for successive use.

Separation of the oil-in-water emulsion

First, 10 ml of Nile red-dyed oil was added to the 500 ml of deionized (DI) water and kept under continuous sonication for 1 hour. Similarly, other emulsions were prepared using different complex aqueous phases, including extremes of pH (pH 1, and pH 12), river water and artificial seawater, without changing the composition of the oil in the respective emulsions. For preparing surfactant stabilized emulsions, the same composition of oil and aqueous phases was maintained, where three types of surfactants: (i) sodium dodecyl sulfate (SDS, a negatively charged surfactant; 1 mM), (ii) cetyl trimethyl ammonium bromide (CTAB, a positively charged surfactant; 1 mM) and (iii) Triton-X solution (a neutral surfactant; 1 mM) were added into the aqueous phase. The prepared emulsions were characterized using fluorescence microscopy and dynamic light scattering study.

Then, the synthesized MASHGO (25 mg) was added to a highly turbid oil-in-water emulsion (5 ml), and the mixture was manually and vigorously agitated for a few minutes. At the end, the magnet was applied to separate the oil-absorbed MASHGO sheets, which eventually provided an optically transparent aqueous phase. The successful separation of oil droplets from the aqueous phase was characterized through visual inspection, fluorescence microscopy and dynamic light scattering study.

Separation of the water in oil emulsion

First, 10 ml of the fluorescein dyed aqueous phase was added to 500 ml of oil and kept under continuous sonication for 1 hour. Eventually, a highly turbid solution of the water-in-oil emulsion was formed. Similarly, the emulsions were prepared in different aqueous environments which include extremes of pH (pH 1, pH 12), river water and artificial seawater with the same composition as the emulsion. For the surfactant stabilized emulsion, aqueous phases were individually contaminated with three types of surfactants—including SDS (1 mM), CTAB (1 mM) and Triton-X solution (1 mM) prior to preparing water-in-oil emulsions. All emulsions were characterized by visual inspection, fluorescence microscopy and dynamic light scattering study.

Thereafter, the same MASHGO (50 mg) was added to the 10 ml water-in-oil emulsion, followed by manual agitation for a minute. MASHGO helped in capturing water droplets from the oil phase by forming a magnetically active 'Pickering-type' aqueous droplet. This droplet was separated by the application of an external magnet and eventually, a water-free oil phase was obtained (see the main text for more details).

Conflicts of interest

There are no conflicts to declare.

Acknowledgements

We acknowledge the financial support from the Department of Science and Board of Research in Nuclear Sciences (BRNS) (34/20/31/2016-BRNS, DAE-YSRA) and Ministry of Electronics and Information Technology (grant no. 5(9)/2012-NANO). We thank CIF and the Department of Chemistry, Indian Institute of Technology, Guwahati, for their generous help. Avijit Das and Kousik Maji are thankful to the CSIR and IITG respectively, for their doctoral fellowships.

References

1 V. Georgakilas, J. N. Tiwari, K. C. Kemp, J. A. Perman, A. B. Bourlinos, K. S. Kim and R. Zboril, *Chem. Rev.*, 2016, **116**, 5464.
2 B. Han, Y. L. Zhang, L. Zhu, Y. Li, Z. C. Ma, Y. Q. Liu, X. L. Zhang, X. W. Cao, Q. D. Chen, C. W. Qiu and H. B. Sun, *Adv. Mater.*, 2019, **31**, 1806386.
3 R. Rauti, M. Medelin, L. Newman, S. Vranic, G. Reina, A. Bianco, M. Prato, K. Kostarelos and L. Ballerini, *Nano Lett.*, 2019, **19**, 2858.
4 K. Zhou, P. Yu, X. Shi, T. Ling, W. Zeng, A. Chen, W. Yang and Z. Zhou, *ACS Nano*, 2019, **13**, 9595.
5 L. Shi, C. Mu, T. Gao, W. Chai, A. Sheng, T. Chen, J. Yang, X. Zhu and G. Li, *J. Am. Chem. Soc.*, 2019, **141**, 8239.
6 X. M. Li, D. Reinhoudt and M. C. Calama, *Chem. Soc. Rev.*, 2007, **36**, 1350.
7 S. Wang, K. Liu, X. Yao and L. Jiang, *Chem. Rev.*, 2015, **115**, 8230.
8 B. Su, Y. Tian and L. Jiang, *J. Am. Chem. Soc.*, 2016, **138**, 1727.
9 C. Peng, Z. Chen and M. K. Tiwari, *Nat. Mater.*, 2018, **17**, 355.
10 V. Jokinen, E. Kankuri, S. Hoshian, S. Franssila and R. H. A. Ras, *Adv. Mater.*, 2018, **30**, 1705104.
11 H. B. Jiang, Y. L. Zhang, D. D. Han, H. Xia, J. Feng, Q. D. Chen, Z. R. Hong and H. B. Sun, *Adv. Funct. Mater.*, 2014, **24**, 4595.
12 L. Xu, G. Xiao, C. Chen, R. Li, Y. Mai, G. Sun and D. Yan, *J. Mater. Chem. A*, 2015, **3**, 7498.
13 J. N. Wang, Y. L. Zhang, Y. Liu, W. Zheng, L. P. Lee and H. B. Sun, *Nanoscale*, 2015, **7**, 7101.

14 K. Jayaramulu, K. Kumara, R. Datta, C. Rçsler, M. Petr, M. Otyepka, R. Zboril and R. A. Fischer, *Angew. Chem., Int. Ed.*, 2016, **55**, 1178.
15 J. Gu, H. Fan, C. Li, J. Caro and H. Meng, *Angew. Chem., Int. Ed.*, 2019, **58**, 5297.
16 J. Wang, F. Han, B. Liang and G. Geng, *J. Ind. Eng. Chem.*, 2017, **54**, 174.
17 T. Yu, F. Halouane, D. Mathias, A. Barras, Z. Wang, A. Lv, S. Lu, W. Xu, D. Meziane, N. Tiercelin, S. Szunerits and R. Boukherroub, *Chem. Eng. J.*, 2020, **384**, 123339.
18 J. Wang and Y. Zheng, *Sep. Purif. Technol.*, 2017, **181**, 183–191.
19 Z. Lei, Y. Deng and C. Wang, *J. Mater. Chem. A*, 2018, **6**, 3258.
20 H. Zhu, D. Chen, W. An, N. Li, Q. Xu, H. Li, J. He and J. Lu, *Small*, 2015, **11**, 5222.
21 C. Ruan, K. Ai, X. Li and L. Lu, *Angew. Chem., Int. Ed.*, 2014, **53**, 5556.
22 Y. Zhao, J. Fang, H. Wang, X. Wang and T. Lin, *Adv. Mater.*, 2010, **22**, 707.
23 L. Zhang, J. Wu, Y. Wang, Y. Long, N. Zhao and J. Xu, *J. Am. Chem. Soc.*, 2012, **134**, 9879.
24 L. P. Xu, X. Wu, J. Meng, J. Peng, Y. Wen, X. Zhanga and S. Wang, *Chem. Commun.*, 2013, **49**, 8752.
25 Y. E. Miao, H. K. Lee, W. S. Chew, I. Y. Phang, T. Liu and X. Y. Ling, *Chem. Commun.*, 2014, **50**, 592.
26 H. K. Lee, Y. H. Lee, I. Y. Phang, J. Wei, Y. E. Miao, T. Liu and X. Y. Ling, *Angew. Chem.*, 2014, **126**, 5154.
27 C. Duan, T. Zhu, J. Guo, Z. Wang, X. Liu, H. Wang, X. Xu, Y. Jin, N. Zhao and J. Xu, *ACS Appl. Mater. Interfaces*, 2015, **7**, 10475.
28 S. Huang, Y. Zhang, J. Shi and W. Huang, *ACS Sustainable Chem. Eng.*, 2016, **4**, 676.
29 Y. Song, J. Zhou, J. B. Fan, W. Zhai, J. Meng and S. Wang, *Adv. Funct. Mater.*, 2018, **28**, 1802493.
30 H.-J. Chen, T. Hang, C. Yang, G. Liu, D. Lin, J. Wu, S. Pan, B. Yang, J. Tao and X. Xie, *Nanoscale*, 2018, **10**, 1978.
31 M. Tenjimbayashi, S. Samitsu and M. Naito, *Adv. Funct. Mater.*, 2019, **29**, 1900688.
32 X. Zhuo and S. Troels, *Angew. Chem., Int. Ed.*, 2019, **58**, 11952.
33 D. Parbata and U. Manna, *Chem. Sci.*, 2017, **8**, 6092–6102.
34 A. M. Rather, N. Jana, P. Hazarikaa and U. Manna, *J. Mater. Chem. A*, 2017, **5**, 23339.
35 W. Wang, B. Tang, B. Ju, Z. Gao, J. Xiu and S. Zhang, *J. Mater. Chem. A*, 2017, **5**, 958.
36 J. Gu, H. Fan, C. Li, J. Caro and H. Meng, *Angew. Chem., Int. Ed.*, 2019, **58**, 5297.
37 S. Yuan, J. Zhu, Y. Li, Y. Zhao, J. Li, P. V. Puyveldea and B. V. Bruggen, *J. Mater. Chem. A*, 2019, **7**, 2723.
38 X. Dong, S. Gao, J. Huang, S. Li, T. Zhu, Y. Cheng, Y. Zhao, Z. Chen and Y. Lai, *J. Mater. Chem. A*, 2019, **7**, 2122.
39 R. Qu, Y. Liu, W. Zhang, X. Li, L. Feng and L. Jiang, *Chem. Sci.*, 2019, **10**, 4089.
40 L. Kang, J. Li, J. Zeng, W. Gao, J. Xu, Z. Cheng, K. Chen and B. Wang, *J. Mater. Chem. A*, 2019, **7**, 16447.
41 J. D. McLean and P. K. Kilpatrick, *J. Colloid Interface Sci.*, 1997, **189**, 242.
42 B. P. Binks and R. Murakami, *Nat. Mater.*, 2006, **5**, 865.
43 W. S. Hummers Jr and R. E. Offeman, *J. Am. Chem. Soc.*, 1958, **80**, 1339.